

Direct Fourier Method in 3D PET Using Accurately Determined Frequency Sample Distribution

Yingbo Li, Anton Kummert, and Hans Herzog

Abstract—In this paper the frequency sample distribution in the reconstructed 3D object spectrum in 3D PET is investigated and accurately determinable by means of the here presented approach. It emerges from Fourier transform of both non-oblique and oblique 2D parallel projections. Direct Fourier method (DFM) is applied for the reconstruction due to its speed advantage. Simulation studies are accomplished to verify the imposed assertion.

I. INTRODUCTION

COMPUTED tomography (CT) is an essential imaging technique in clinical diagnostics, which provides non-invasive insights about the regional physiological processes within human bodies. Among the broad spectrum of tomographic techniques, Positron Emission Tomography (PET) is regarded as the key technique in neuroscience to study the metabolism function in vivo. Here, measurements as coincidence of photon pairs from individual annihilations, approximate the line integrals of the underlying positron-emitting tracer distribution along straight lines of response (LOR) between individual pairs of detectors. Considering that the reconstructed images yield information on positron-emitting tracer distributions, malfunctions which are characteristic for diverse illnesses could then be diagnosed.

Due to the physical nature of the positron's annihilation procedure, PET is intrinsically a three-dimensional (3D) imaging technique as the coincidence detection could occur theoretically along arbitrary 3D directions. To collect as many coincidence events as possible, most of the modern commercial PET scanners nowadays have a cylindrical multi-ring structure, which has a cylindrical surface subdivided into uniform block detector units along both the transverse and axial direction. The thereby originated large axial field of view (FOV) enables achievement of high system sensitivity by accepting the additional cross-plane coincidence events under large range of oblique angles [1]. The involving drawback of such a data acquisition procedure is however the excessive data volume and accordingly the clinically impractical reconstruction time.

To circumvent this difficulty, the direct Fourier method (DFM) applied to the 2D scenario may be a promising solution. First of all, DFM and the classical Fourier slice theorem (FST) have to be reconsidered. The essential step of the 2D DFM is the interpolation procedure from irregularly distributed frequency samples onto the suitably selected Cartesian grid in 2D Fourier domain, enabling the utilization of inverse fast Fourier transform and thereby the speed advantage. Compared with other analytical reconstruction approaches, e.g. the filtered back-projection, the significant advantage of DFM lies in its short reconstruction time. On the other hand, the involved 2D frequency interpolation is also liable to introduce extra artifacts to the reconstructions and results in alleged bad quality respectively.

Although DFM was conventionally proposed for 2D reconstruction scenarios, its adoption for the 3D case is straightforward. Relying on the 3D extension of FST, which relates the 2D Fourier transform of parallel projections with a central plane crossing the 3D Fourier transform of the object at the same spatial angle, the spectral values on a Cartesian arranged frequency grid can be computed by interpolating the spectral values of usually non-uniformly distributed neighboring frequency samples. On closer examination, for the usual cylindrical multi-ring structure of most PET scanners, the 3D interpolation could be even omitted and simplified to a true 2D interpolation operation, which accelerates the reconstruction speed.

In the present paper, the irregular spatial distribution of frequency samples in the reconstructed 3D object spectrums, which are made up of 2D Fourier transforms of parallel projections along various spatial angles, is investigated and accurately determinable. In particular, it is demonstrated that for the cylindrical multi-ring scanner structures only a consecutive 2D interpolation is necessary to be performed in the 3D frequency domain. Finally, simulation studies based on the 3D Shepp-Logan phantom are provided.

II. THE PRINCIPLE OF ANALYTICAL METHODS IN 3D PET

The fundamental analytical concept used for 3D PET is the 3D Radon transform, which relates the continuous projections and the original continuous object via straight line integrals. With the continuous distribution $f(x,y,z)$ defined in 3D physical space domain, the theoretically obtainable projection data $p(u,v,\vartheta,\varphi)$ can be defined as the line-integral of f along a straight line at an azimuthal angle φ and a co-polar angle ϑ , which crosses the perpendicular

Manuscript received April 1, 2006. This work is supported by the German Research Foundation (DFG) under Grant KU 678/10-2.

Y. Li is with the Faculty of Electrical, Information and Media Engineering, University of Wuppertal, Wuppertal, Germany, (phone: 049-202-4391809; fax: 049-202-4391959; e-mail: yingbo@uni-wuppertal.de).

A. Kummert is with University of Wuppertal, Wuppertal, Germany. (e-mail: kummert@uni-wuppertal.de).

H. Herzog is with the Institute of Medicine, Research Centre Jülich, Jülich, Germany, (e-mail: h.herzog@fz-juelich.de).

projection panel at the position u and v . Mathematically, such a 4D projection signal can be described as

$$p(u, v, \vartheta, \varphi) = \int_{-\infty}^{+\infty} \int_{-\infty}^{+\infty} \int_{-\infty}^{+\infty} f(x, y, z) \cdot \delta(u + x \sin \varphi - y \cos \varphi) \cdot \delta(v + x \cos \varphi \sin \vartheta + y \sin \varphi \sin \vartheta - z \cos \vartheta) dx dy dz. \quad (1)$$

In accordance with this mathematical definition, the 3D extension of FST implies that the 2D Fourier transform of the projection data $p(u, v, \vartheta, \varphi)$ with respect to the variables u and v at a certain spatial angle pair (ϑ, φ) corresponds to a central plane crossing the 3D Fourier transform of the object $f(x, y, z)$ with respect to x, y , and z at the same spatial angles. This relationship is illustrated in Fig. 1, where the 2D Fourier transform of the projection data with respect to u and v , $P(j\omega_u, j\omega_v, \vartheta, \varphi)$, is depicted as a dark shaded disc.

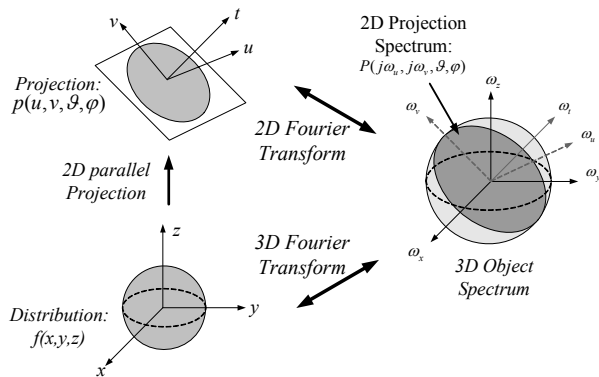


Fig. 1. Schematic illustration of the extended 3D Fourier slice theorem.

In view of the extended 3D FST, it is apparent that theoretically the continuous object spectrum could be entirely recovered by acquiring continuous 2D projection spectrum panels of various spatial angles. On the other hand, for the continuous case, not all available spatial angles must be taken into account to grant the completeness of the recovered object spectrum. Rather, only a subset of all possible spatial angles needs to be considered, which enable the shaded disc shown in Fig. 1 to about-face itself exactly once so as to fully recover the object spectrum.

III. SPATIAL ARRANGEMENT OF FREQUENCY SAMPLES IN THE RECONSTRUCTED 3D OBJECT SPECTRUM

In 3D PET systems, the reconstructed 3D object spectrum is actually composed of frequency samples since the acquired measurements are merely estimated samples of the underlying continuous projection signal $p(u, v, \vartheta, \varphi)$. Furthermore, due to the multi-ring block-detector structure and the capability of collecting cross-plane coincidence events, the spatial distribution of the frequency samples among the 3D object spectrum could be constituted by revolving a 2D Cartesian lattice of the Fourier transform, $P(j\omega_u, j\omega_v, \vartheta, \varphi)$, of various oblique angles consecutively. In Fig. 2, the constitution of such a frequency sample distribution is schematically illustrated. On the left hand side, the revolving 2D Cartesian lattice has no tilt angle with respect to the ω_z -axis, which corresponds to the coincidence

events in transverse planes; whereas on the right hand side the revolving 2D Cartesian lattice tilts with respect to the rotation axis (ω_z -axis), which correlates with the cross-plane coincidence events. Although the sampling along the transverse direction actually has a fan-beam pattern, it could be treated as a parallel-beam pattern effectively after an arc-correction, which implies equidistantly arranged samples along the transverse direction. Due to the PET scanner geometry, the measurable samples along the axial direction are indeed equidistantly arranged, thus 2D fast Fourier transform (FFT) can be utilized to compute the 2D Cartesian frequency samples on projection panels economically. For the case that the rotating projection panel tilts with respect to the rotation axis (z -axis), the confined spatial region, in which the 3D object spectrum could not be recovered, resembles a head-to-head adhered truncated double-cone, which is also indicated on the right hand side of Fig. 2 [2].

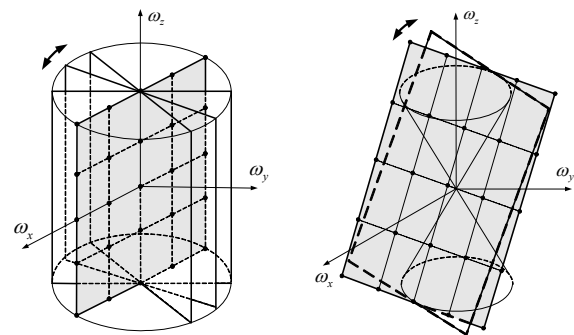


Fig. 2. Schematic illustration of the constitution of a frequency sample arrangement in the reconstructed 3D object spectrum

Intrinsically, the frequency samples in the thereby reconstructed 3D object spectrum have various densities in various regions. The density of the frequency samples depends generally on the oblique angle with respect to the ω_z -axis. More precisely, presumed that the PET scanner has a cylindrical multi-ring structure, it could be mathematically proved that the frequency samples along the axial direction, which are computed by using the FFT algorithm, fall exactly in the same set of transverse planes (equidistant planes orthogonal to the ω_z -axis) in the reconstructed object spectrum, no matter how large the oblique angle is. Thereupon the accurate arrangement of the frequency samples in various transverse planes could be determined. In Fig. 3, the spatial location of measurable projection samples with respect to the z -axis is schematically illustrated. With the assumption that the unit distance between the adjacent transverse planes is Δu , one can easily recognize that the unit distance between projection samples lying on inclined projection panels is actually $\cos \alpha \cdot \Delta u$ with α as the inclination angle relative to the z -axis.

Regarding that the frequency samples in the Fourier transformed 2D projection panel are computed by using the FFT algorithm, the distance between the frequency samples on the inclined projection panel then is $2\pi/(N \cdot \Delta u \cdot \cos \alpha)$, where N is the total number of projection samples and usually FFT-friendly. Respectively, the distance between the

frequency samples on the non-inclined projection panel is $2\pi/(N\cdot\Delta u)$. Since the projection panels all have exactly the same origin in 3D space domain, regardless of the tilt angle, it can be claimed that the frequency samples on the Fourier transformed inclined projection panel have exactly the same axial coordinate (ω_z -coordinate) as the frequency samples lying on the Fourier transformed non-inclined projection panel due to $2\pi/(N\cdot\Delta u\cdot\cos\alpha)\cdot\cos\alpha = 2\pi/(N\cdot\Delta u)$, shown in Fig. 4. This means, no matter how the frequency samples are acquired, they are located always in the same transverse planes among the reconstructed 3D object spectrum.

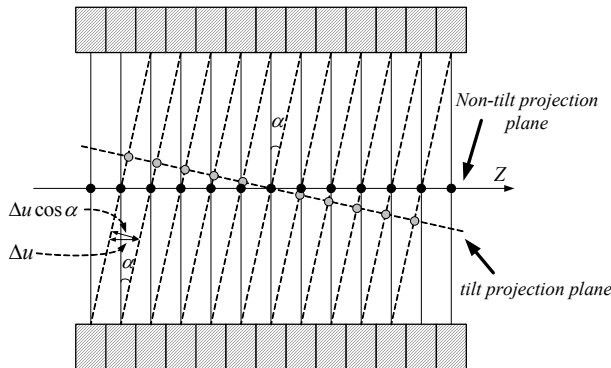


Fig. 3. Schematic illustration of the location of projection samples along the z -axis for a PET scanner with cylindrical multi-ring detector structure.

For precise determination of the frequency sample distribution in individual transverse planes, the relative axial position of single transverse planes is apparently a major influencing factor. Observation of Fig. 4 reveals that the wider a transverse plane is away from the spectral origin, the further away the frequency samples, originating from inclined projection panels, are located from the ω_z -axis. The mathematical statement of this dependence is given by $(n\cdot 2\pi)/(\Delta u\cdot\tan\alpha)$, where $n\cdot(2\pi/\Delta u)$ depicts the spectral distance of the transverse plane from the spectral origin.

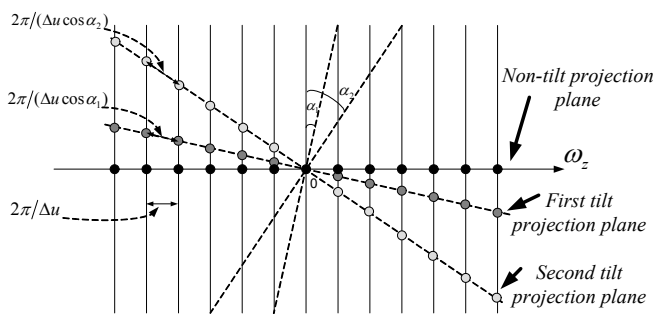


Fig. 4. Schematic illustration of the location of frequency samples along the ω_z -axis in the reconstructed 3D object spectrum.

In fact, each single frequency node illustrated in Fig. 4 represents in true 3D scenario a series of equidistantly arranged frequency samples on a straight line. Since the 3D object spectrum could be recovered by revolving oblique and non-oblique panels, the accurate position of irregularly distributed frequency samples in each transverse plane could be straightforward determined by revolving several queues of frequency nodes simultaneously, whereas each queue of

frequency nodes reside equidistantly on one of the parallel straight lines. The displacements between adjacent parallel lines depend on the oblique angle and the transverse plane's location. Additionally, if a transverse plane exactly crosses the spectral origin, the frequency samples originating from an oblique projection panel overlap totally with the frequency samples originating from non-oblique projection panels. Fig. 5 exemplifies all the situations schematically.

At first, the 3D situation without inclined projection panels is regarded, which matches exactly the 2D scenario layer-wise. For a certain rotation angle, the frequency sample distributions in all transverse planes arise from revolving a single queue of frequency samples and have a uniform polar pattern, see Fig. 5a and 5b. Normally, presumed that an adequate number of rotation angles is chosen, the frequency sample density in the central region of each plane is sufficiently high for successive interpolation procedures, while the poorly low sample density in the border area causes in case of DFM most artifacts in the reconstructed images. On the contrary, for an exemplary situation that besides the non-inclined projection panel one inclined projection panel is also available, the accurate position of highly non-uniformly distributed frequency samples in a certain transverse plane could be obtained by rotating the frequency sample structure akin to ones shown in Fig. 5c and 5e. Because of the geometrical symmetry of PET scanners, the inclination angles exist always by pairs, and so the three queues of frequency samples. The displacements between queues are dependent on the involved transverse plane's location and can be determined according to the scanner geometry. Thereupon the transverse plane shown in Fig. 5c is obviously lying nearer to the spectral origin than the one shown in Fig. 5e.

Generally speaking, taking inclined projection panels into account always leads to an increase of the frequency sample density in various transverse planes in the reconstructed object spectrum. However, depending on the spatial location of the transverse planes the benefit in different regions of the planes fluctuates considerably. For transverse planes near the spectral origin, the displacements are relatively small. Accordingly, the additional frequency samples concentrate predominantly in the central region so that an even higher density comes about; whereas in the border region the density changes only slightly, see Fig. 5d. For transverse planes comparatively far from the spectral origin, the predominant concentration of the additional frequency samples shifts outwards, shown in Fig. 5f. According to this fact, the frequency sample density in the border area of planes increases and minimizes the artifacts effectively. Contrariwise, in the central region of transverse planes the benefit is less significant. As the density is there already sufficiently high, the entire reconstruction quality does not suffer much from it. A particular case worth mentioning represents the exact median transverse plane crossing the spectral origin. The frequency samples in it, despite

incorporating the oblique projection panels, still have a quasi-uniform polar distribution, similar in appearance to the usual frequency sample distribution known from 2D scenarios. This is due to the effect of overlapping, caused by the PET scanner geometry. Nevertheless, regarding the artifact elimination the additional frequency samples are any way helpful and welcome.

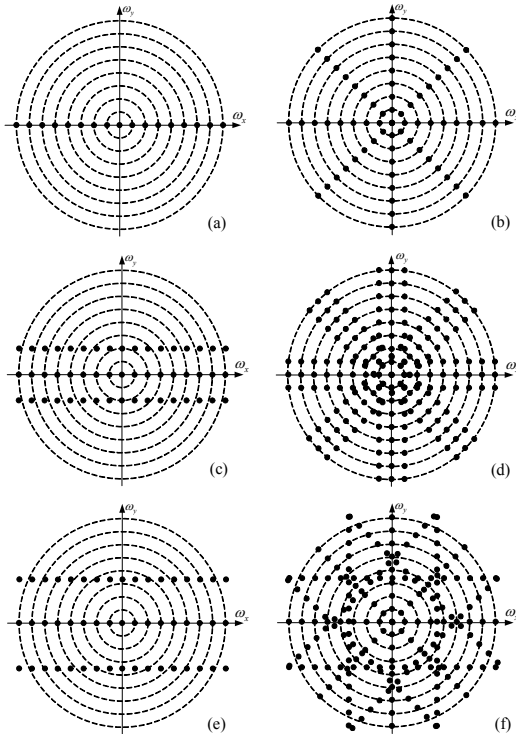


Fig. 5. Determining the position of irregularly distributed frequency samples in individual transverse planes for an exemplary scenario.

IV. SIMULATION STUDIES

To verify the imposed assertion, simulation studies were performed. Indeed, experimental phantom measurement via a real 3D PET scanner was also accomplished. Yet due to the inherently existing large proportion of noise among the real measurements the precise quantification is relatively difficult to reach and possesses little significance, hence simulation studies are here preferred. The required simulator is implemented in the programming language C++.

During the simulation, an analytic Shepp-Logan phantom is used, which is a superposition of ellipses representing the human brain structure. To constitute a true 3D structure, several planes containing the 2D Shepp-Logan phantom of different dimensions are stacked together to form the 3D structure. The corresponding 2D parallel projections at various spatial angles could then be computed by means of a self-developed, analytically accurate modeling of the PET system probability matrix. After adjusting the dimension of the 2D projection panels to be FFT-friendly, FFT algorithm could be utilized to perform the Fourier transform of projections. An irregular distribution of frequency samples among the recovered 3D object spectrum could then be generated by merging diverse Fourier transformed 2D

projection data together. The 2D interpolation procedure on individual transverse planes is implemented by using the 2D Inverse Distance Weighting (IDW) interpolation method.

In Fig. 6 selected layers of the original and reconstructed phantom object are illustrated. The original phantom object has a dimension of $128 \times 128 \times 32$, i.e. totally 32 layers. To imitate the human brain, on each layer the phantoms are chosen with varying dimensions. In this simulation, the size of the phantom object on the topmost and lowermost layer is merely 60% of the phantom object size on the central layer. The increase or decrease of the phantom object size occurs gradually. Fig. 6a shows the original phantom image in the central plane, while Fig. 6b shows the reconstructed image. In Fig. 6c and 6d the original and reconstructed phantom image in the topmost layer are displayed, respectively. The simulation results confirm the correctness of the frequency sample distribution in the reconstructed object spectrum.

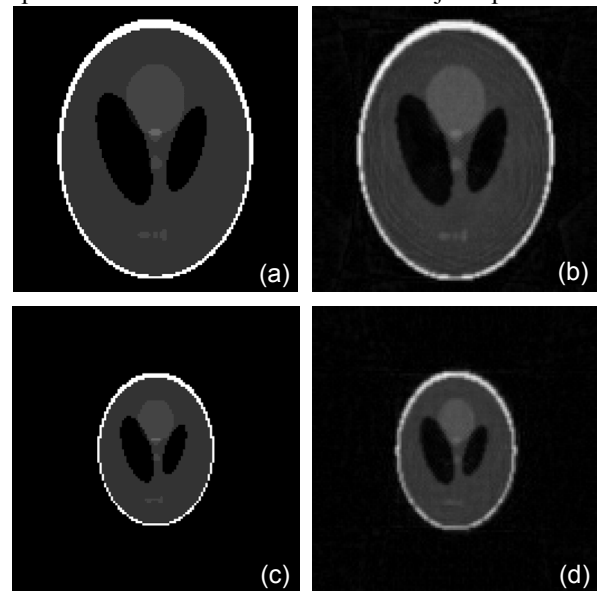


Fig. 6. Selected layers of the original and reconstructed 3D phantom object.

V. CONCLUSION

In this work a method for accurately determining the frequency sample location in the reconstructed object spectrum is presented. DFM is definitely capable of taking advantage of additional frequency samples from inclined projection panels. Simulation studies confirmed this assertion. A particular feature in 3D PET is the incompleteness of projection data on inclined projection panels, which brings up difficulties for DFM. A suitable solution, e.g. 3D reprojection (3DRP) is already imposed. However, here it is not considered, since otherwise it would go beyond the scope of the present paper.

REFERENCES

- [1] B. Bendriem, D. Townsend, *The Theory and Practice of 3D PET* (Book style). Kluwer, AH: Dordrecht, 2001.
- [2] Y. Li, A. Kummert, F. Boschen, and H. Herzog, "Investigation on projection signals in 3D PET systems (Presented Conference Paper style)," presented at the 2005 Int. Conf. on Biomedical Engineering, Singapore.